Characterization and Electrochromic Properties of Ultrathin Films Self-Assembled from Poly(diallyldimethylammonium) Chloride and Sodium Decatungstate

Isamu Moriguchi† and Janos H. Fendler*,‡

Department of Applied Chemistry, Faculty of Engineering, Nagasaki University, 1-14 Bunkyo-machi, Nagasaki 852, Japan, and Center of Advanced Material Processing, Clarkson University, P.O. Box 5814, Potsdam, New York 13699

Received March 4, 1998. Revised Manuscript Received May 28, 1998

Poly(diallyldimethylammonium) chloride (**P**) and sodium decatungstate (**W**) were layer-by-layer self-assembled onto quartz, mica, and ITO-electrode substrates (S). The self-assembled films, S-(**P**/**W**)$_n$, were characterized by absorption spectrophotometry, reflectivity, cyclic voltammetry and scanning force microscopy (AFM). The electrochemical properties of the S-(**P**/**W**)$_n$ films were found to differ from those in which the polyelectrolyte remained at the outermost layer, i.e., S-(**P**/**W**)$_n$/**P**. Photoelectrochemical measurements provided evidence for the electrochromic and photoelectrochromic behavior of these films.

Introduction

The versatility and relative ease of experimentation have prompted the increased interest in the colloid chemical approach to advanced materials preparation.[1,2] Syntheses of nanoparticles and their organization into two-dimensional arrays and three-dimensional networks have laid the foundations for device construction.[3−6] In particular, ultrathin films have been formed from appropriately coated and/or derivatized metallic, semiconducting, magnetic, and ferroelectric nanoparticles as well as from inorganic nanoplatelets by the Langmuir−Blodgett technique[7−19] and by self-assembly.[4,20−26]

Self-assembly is deceptively simple. It involves the sequential adsorption of oppositely charged polyelectrolytes,[2,10,22] polyelectrolytes and nanoparticles,[22,24] polyelectrolytes and graphite oxide,[24,25,27] and polyelectrolytes and clay platelets.[21,28] Attraction of self-assembly is that any number of layers of nanoparticles (or platelets) of any composition can be adsorbed onto a large variety of structurally different substrates in any desired order.

Prompted by the reported multilayer formation of polyoxometalates on electrodes[29−31] and by the recognized beneficial electrochemical,[32−34] photochemical,[35] and catalytic[36−38] properties of nanoparticles prepared from tungstate, vanadate, and molybdate oxides, we have initiated studies for the preparation, characteriza-

† Nagasaki University.

‡ Clarkson University.

(1) Fendler, J. H. *Membrane-Mimetic Approach to Advanced Materials*; Springer-Verlag: Berlin, 1994; Advanced in Polymer Science Series, Vol. 113.

(2) Fendler, J. H.; Meldrum, F. C. *Adv. Mater*. **1995**, *7*, 607.

(3) Kamat, P. V. Native and Surface Modified Semiconductor Nanoclusters. In *Progress in Inorganic Chemistry*; Meyer, G. J., Ed.; John Wiley & Sons Inc.: New York, 1997; Vol. 44; pp 273−343.

(4) *Ultrathin Films based on Layered Inorganic Solids*; Mallouk, T. E., Kim, H.-N., Ollivier, P. J., Keller, S. W., Eds.; Pergamon Press: Oxford, 1996; Vol. 7, p 189.

(5) Weller, H. *Angew. Chem., Int. Ed. Eng.* **1996**, *35*, 1079−1081.

(6) Freeman, R. G.; Fox, A. P.; Keating, C. D.; Musick, M. D.; Natan, M. J. *Langmuir* **1996**, *12*, 2353−2361.

(7) Zhao, X. K.; Xu, S.; Fendler, J. H. *J. Phys. Chem*. **1994**, *98*, 8827.

(8) Moriguchi, I.; Tanaka, I.; Teraoka, Y.; Kagawa, S. *J. Chem. Soc., Chem. Commun*. **1991**, 515.

(9) Moriguchi, I.; Hosoi, K.; Nagaoka, H.; Tanaka, I.; Teraoka, Y.; Kagawa, S. *J. Chem. Soc., Faraday Trans*. **1994**, *90*, 349.

(10) Kotov, N. A.; Meldrum, F. C.; Fendler, J. H. *J. Phys. Chem*. **1994**, *98*, 8827.

(11) Tian, Y.; Wu, C.; Fendler, J. H. *J. Phys. Chem*. **1994**, *98*, 4913.

(12) Moriguchi, I.; Nii, H.; Hanai, K.; Nagaoka, H.; Teraoka, Y.; Kagawa, S. *Colloids Surf*. **1995**, *103*, 173.

(13) Ichinose, I.; Kimizuka, N.; Kunitake, T. *J. Phys. Chem*. **1995**, *99*, 3736.

(14) Zhao, X. K.; Fendler, J. H. *Chem. Mater*. **1991**, *3*, 168.

(15) Zhao, X. K.; Xu, S.; Fendler, J. H. *Langmuir* **1991**, *7*, 520.

(16) Yang, J.; Fendler, J. H. *J. Phys. Chem*. **1995**, *99*, 5505.

(17) Moriguchi, I.; Maeda, H.; Teraoka, Y.; Kagawa, S. *J. Am. Chem. Soc*. **1995**, *117*, 1139.

(18) Tian, Y.; Fendler, J. H. *Chem. Mater*. **1996**, *8*, 969.

(19) Moriguchi, I.; Maeda, H.; Teraoka, Y.; Kagawa, S. *Chem. Mater*. **1997**, *9*, 1050.

(20) Iler, R. K. *J. Colloid Inetrface Sci*. **1966**, *21*, 569.

(21) Kleinfeld, E. R.; Ferguson, G. S. *Science* **1994**, *265*, 370.

(22) Keller, S. W.; Kim, H. N.; Mallouk, T. E. *J. Am. Chem. Soc*. **1994**, *116*, 8817. Keller, S. W.; Johnson, S. A.; Brigham, E. S.; Yonemoto, E. H.; Mallouk, T. E. *J. Am. Chem. Soc*. **1995**, *117*, 12879. Kim, H.-N.; Keller, S. W.; Mallouk, T. E.; Smitt, J.; Decher, G. *Chem. Mater*. **1997**, *9*, 1414.

(23) Freeman, R. G.; Graber. K. C.; Allison, K. J.; Bright, R. M.; Davis, J. A.; Guthrie, A. P.; Hommer, M. B.; Jackson, M. A.; Smith, P. C.; Walter, D. G.; Natan, M. J. *Science* **1995**, *267*, 1629.

(24) Kotov, A. N.; Dekang, I.; Fendler, J. H. *J. Phys. Chem*. **1995**, *99*, 13065.

(25) Fendler, J. H. *Chem. Mater*. **1996**, *8*, 1616.

(26) Lvov, Y.; Ariga, K.; Ichinose, I.; Kunitake, T. *Langmuir* **1996**, *12*, 3038.

(27) Kotov, N. A.; Haraszti, T.; Turi, L.; Zavala, G.; Geer, R. E.; Dékány, I.; Fendler, J. H. *J. Am. Chem. Soc*. **1997**, *119*, 6821.

(28) Kleinfeld, E. R.; Ferguson, G. S. *Mater. Res. Soc. Symp*. **1995**, *369*, 697. (d) Kleinfeld, E. S.; Ferguson, G. S. *Chem. Mater*. **1996**, *8*, 1575.

(29) Moriguchi, I.; Hanai, K.; Hoshikuma, A.; Teraoka, Y.; Kagawa, S. *Chem. Lett*. **1994**, 691.

(30) Ingersoll, D.; Kulesza, J. P.; Faulkner, L. R. *J. Electrochem. Soc*. **1994**, *141*, 140.

(31) Kuhn, A.; Anson, F. C. *Langmuir* **1996**, *12*, 5481.

S0897-4756(98)00127-6 CCC: $15.00
Published on Web 07/25/1998

tion, and utilization of ultrathin films self-assembled from polyelectrolytes and sodium decatungstate. Decatungstate ions, $(W_{10}O_{32})^{4-}$, have demonstrated both electrochromic and photochromic behavior: colorless or pale yellow aqueous solution of $(W_{10}O_{32})^{4-}$ could reversibly be reduced to a blue solution of $(W_{10}O_{32})^{5-}$ by an electron.[35,38]

Preparation and characterization of composite ultrathin electrochromic and photochromic films, by the layer-by-layer self-assembly of poly(diallyldimethylammonium chloride), **P**, and sodium decatungstate, **W**, onto solid substrates (mica, quartz slide, or indium tin oxide, ITO, coated glass), are the subject of the present report.

Experimental Section

Materials. Sodium tungstate, $Na_2WO_3 \cdot 2H_2O$, and a 20 wt % aqueous solution of poly(diallyldimethylammonium chloride), **P**, were obtained from Baker&Adamson Co. Ltd. and Aldrich Chemical Co., respectively. All of the other chemicals (hydrochloric acid, sulfuric acid, hydrogen peroxide, sodium chloride) were reagent grade (J. T. Baker, Inc.) and were used as received. Water was purified by using a Millipore Milli-Q filter system provided with a 0.22 μm Millistack filter at the outlet.

An aqueous solution of sodium decatungstate, **W**, was prepared by the acidification of 0.1 M $Na_2WO_3 \cdot 2H_2O \cdot Na$ (to pH = 2.5 by the dropwise addition of 1 M HCl under vigorous stirring).[39] It was identified by its characteristic absorption maximum around 323 nm, which corresponds to the oxygen-to-tungsten charge-transfer band.[35,40,41]

Self-Assembly of the S-(P/W)$_n$/P Films. Quartz, ITO-coated glass (on one side only), and mica were used substrates, S, for the self-assembly. The surface of the quartz and the ITO-coated glass was cleaned by immersion into a H_2SO_4:H_2O_2 = 7:3 (v/v) solution for a few minutes followed by washing copiously by Milli-Q water. Mica was freshly cleaved with an adhesive tape just prior to use.

Self-assembly of an ultrathin film of one sandwich layer on a substrate, containing a nanolayer of **P** and a nanolayer of **W**, S-(**P**/**W**), involved the following steps: (i) immersion of S into a 20 mM aqueous **P** solution, kept at pH = 2.5 (no buffer, ionic strength = 0.02 M), for 5 min; (ii) rinsing for 10 s with a dilute aqueous HCl solution (pH = 2.5); (iii) immersion into a 10 mM aqueous **W** solution, kept at pH = 2.5, for 5 min; (iv) washing with a dilute aqueous HCl solution (pH = 2.5). Each washing was followed by drying by a stream of N_2 gas for 30 s. A subsequent *n* number of sandwich layers, to produce an ultrathin film containing alternating *n* layers of **P** and *n* layers of **W**, S-(**P**/**W**)$_n$, were prepared by repeating steps (i), (ii), (iii), and (iv) *n* times. The schematics of the self-assembly of an S−(P−W)$_n$ film are illustrated in Figure 1. In some cases thin films were prepared in which the polyelectrolyte remained at the outermost layer, i.e., S-(**P**/**W**)$_n$/**P**.

Instrumental Analysis. UV−vis absorption spectra of quartz-, mica-, and ITO-supported films were recorded on a diode array spectrometer (Hewlett-Packard Model 8452A). The mica used for UV−vis absorption measurements was carefully cleaved (no pieces of mica could be detected on the surface visually), and the edge of mica plate was sealed with epoxy resin to prevent water from intercalating into the mica interlayers. The uncoated side of ITO glass was marked by vinyl tape during the self-assembly of **P** and **W**. This tape was removed prior to taking absorption spectra for monitoring the S-(**P**/**W**)$_n$ film formation so that self-assembly only on the ITO-coated side of the substrate was recorded.

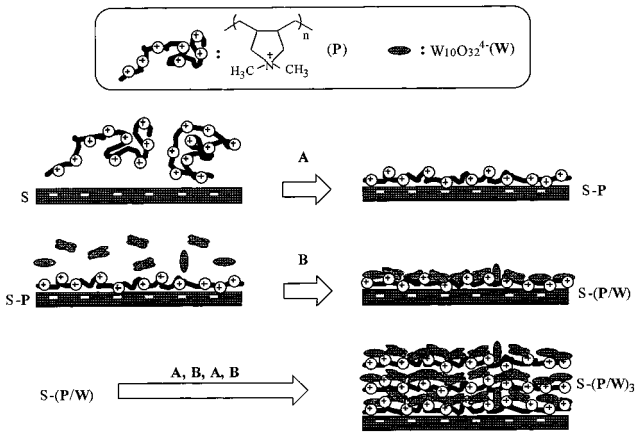

Figure 1. Schematics of the layer-by-layer self-assembly of P and W.

Atomic force microscopic (AFM) images were taken on mica-supported films using a Topometrix Explorer 2000 scanning probe microscope with a 2 μm scanner and silicon nitride tips (spring constant = 34−44 Nm^{-1}, F_0 = 176 kHz). AFM images were taken in air in the noncontact mode and were examined at least in three different sites in a given sample.

Thicknesses of the self-assembled films (formed on the half side of quartz and ITO glass plates) were evaluated by incident-angle-dependent-reflectivity measurements.[7] The uncoated side of substrate was brought into optical contact with the glass prism by an index matching oil (n = 1.518 ± 0.0005). A He−Ne laser (13 mW, 6328 Å) was tightly mounted on a precision rotating stage. P-polarized He−Ne light (13 mW, 6328 Å) was directed to the surface of the film on the substrates. The angle of incident light was changed by sliding the post in horizontal direction parallel to the surface without affecting the optical geometry. The intensity of the reflected light was measured by means of a Spectra Physics Model 404 silicon photocell power meter. The reflectivity was obtained as the intensity ratio of the reflected to incident light.

The voltammetric and chronoamperometric experiments were carried out by an EG&G Princeton Applied Research Model 273 potentiostat galvanostat at ambient temperature (22 ± 2 °C) in a 0.1 M aqueous NaCl solution (pH = 2.5) that has been bubbled with N_2 gas for more than 20 min before measurements. Electrical contact with the ITO electrode was made by means of liquid silver completely sealed by epoxy resin to prevent it from coming in contact with the electrolyte. ITO electrodes coated by the self-assembled films were placed in solution with a Pt counter electrode and the SCE reference electrode. Cyclic voltammograms (CVs) were taken in the range from +700 to −900 mV. The amount of **W** per unit area was determined by integrating the area of voltammetric *i-E* curves. Formal potentials (E°′) were determined as the average of cathodic and anodic peak potentials in cyclic voltammograms. Spectroelectrochemical experiments were performed by measuring absorption spectra and monitoring the absorbance at 780 nm (−0.4 V) and 650 nm (−0.8 V) as a function of time during chronoamperometry with potential steps of 0 V → −0.4 V and 0 V → −0.8 V as well as +0.4 V ⇌ −0.8 V.

Results and Discussion

Preparation and Characterization of S-(P/W)$_n$ and S-(P/W)$_n$/P Ultrathin Films. Quartz-supported

(32) Keita, B.; Nadjo, L.; Krier, G.; Muller, J. F. *J. Electroanal. Chem.* **1987**, *223*, 287.
(33) Keita, B.; Nadjo, L. *J. Electroanal. Chem.* **1988**, *240*, 325.
(34) Kasem, K. K.; Schultz, F. A. *Can. J. Chem.* **1995**, *73*, 858.
(35) Yamase, T.; Takabayashi, N.; Kaji, M. *J. Chem. Soc., Dalton Trans.* **1984**, 793.
(36) Okuhara, T.; Nishimura, T.; Ohashi, K.; Misono, M. *Chem. Lett.* **1990**, 1201.
(37) Toth, J. E.; Anson, F. C. *J. Am. Chem. Soc.* **1989**, *111*, 2444.
(38) Keita, B.; Nadjo, L. *J. Electroanal. Chem.* **1994**, *33*, 1064. Takabayashi, N.; Yamase, T. *Nippon Kagaku Kaishi* **1984**, 264.
(39) Filowitz, M.; Ho, R. K. C.; Klemperer, W. G.; Shum, W. *Inorg. Chem.* **1979**, *18*, 93.
(40) Ternes, S. C.; Pope, M. T. *Inorg. Chem.* **1978**, *17*, 500.
(41) Chemseddine, A.; Sanchez, C.; Jivage, J.; Launay, J. P.; Fournier, M. *Inorg. Chem.* **1984**, *23*, 2609.

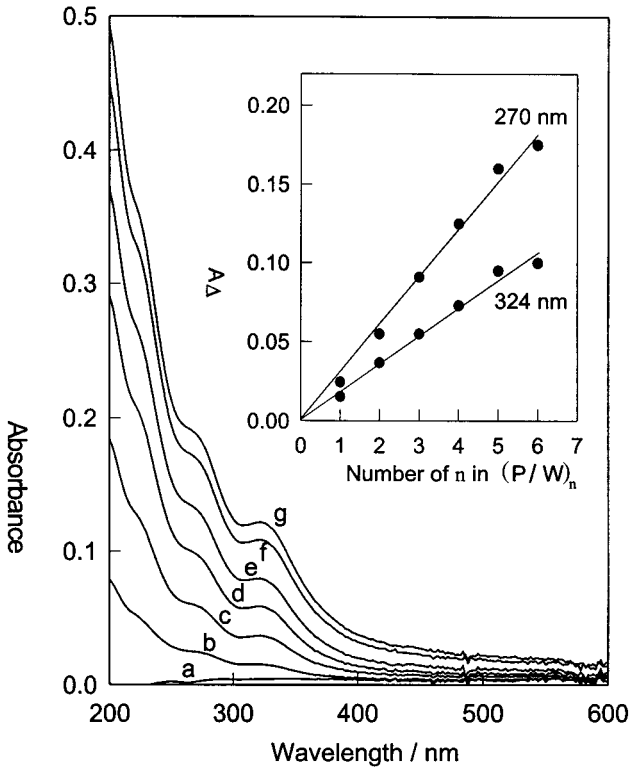

Figure 2. Absorption spectra of a layer of **P** (a) and of self-assembled S-(**P**/**W**)$_n$ films with $n = 1$ (b), $n = 2$ (c), $n = 3$ (d), $n = 4$ (e), $n = 5$ (f), and $n = 6$ (g). The inset shows plots of absorbances at 270 and 324 nm against n.

S-(**P**/**W**)$_n$ films exhibited absorption peaks at 270 and 324 nm (Figure 1),[35,40] substantiating the incorporation of $W_{10}O_{32}^{4-}$ anions into the composite film without any structural alteration. The self-assembly was optimized by monitoring the absorbances as a function of substrate immersion time into **P** and **W** solutions; 5 min of immersion time was found to be ideal for the adsorption of one layer of **P** and one layer of **W**. Absorbances at 270 and 324 nm of quartz-supported S-(**P**/**W**)$_n$ films increased proportionally with increasing n (see the inset of Figure 2) indicating quantitative and reproducible self-assembly. No difference in the absorption spectra was observed for any self-assembled films on mica or on ITO-coated glass ($n = 1-10$ in S-(**P**/**W**)$_n$) prior to and after the adsorption of an additional **P** layer and the absorbances increased linearly with increasing values of n (Figure 3). The amount of **W** adsorbed onto quartz, mica, and ITO-coated glass in one self-assembly step was estimated to be 6.2×10^{-10}, 4.9×10^{-10}, and 2.1×10^{-10} mol cm^{-2}, respectively, by using the reported molar absorbance for **W** ($\epsilon = 1.35 \times 10^4$ dm^3 mol^{-1} cm^{-1}).[42] This value for quartz-supported films is ca. 2−3 times greater than that evaluated from the geometric area of a **W** molecule (64−96 Å^2),[29,42] suggesting that $W_{10}O_{32}^{4-}$ penetrate into and adsorb onto an underlying **P** layer to form a **P**−**W** ion complex.

The thicknesses of S-(**P**/**W**)$_3$/**P**, S-(**P**/**W**)$_5$/**P**, and S-(**P**/**W**)$_7$/**P** films self-assembled onto quartz slides were determined to be 210, 320, and 450 Å, by reflectivity measurements. A good relationship was obtained on plotting the thicknesses of the self-assembled S-(**P**/**W**)$_n$

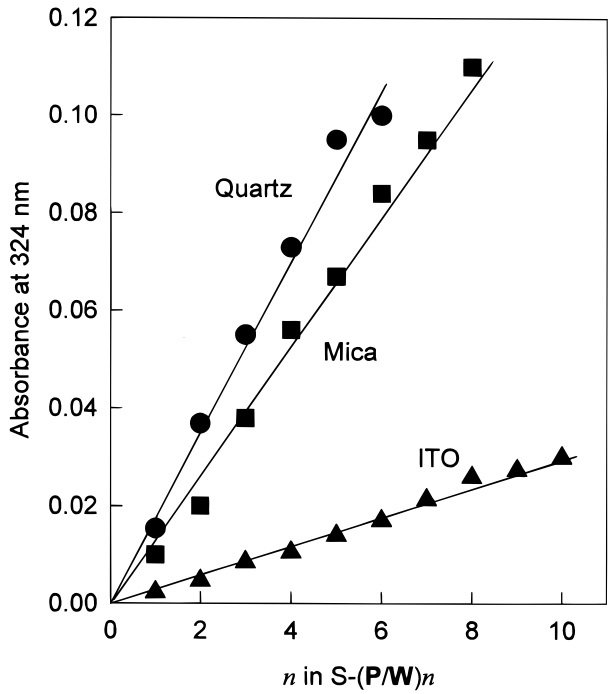

Figure 3. Plots of absorbances at 324 nm against n for self-assembled S-(**P**/**W**)$_n$ films with S = quartz, S = mica, and S = ITO-coated glass.

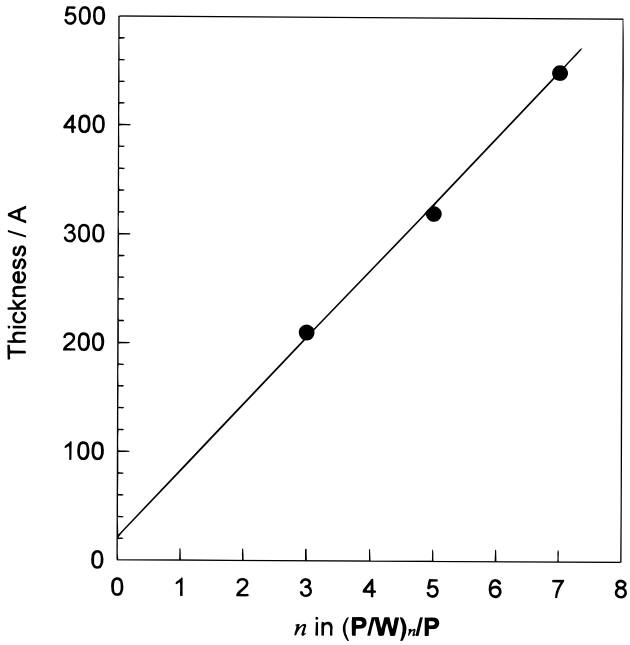

Figure 4. Thickness of the self-assembled S-(**P**/**W**)$_n$ films, as determined by reflectivity measurements.

films, determined by reflectivity measurements, against n (Figure 4). From the slope and intercept of the plot, the thicknesses of the **P**/**W** unit and of the first **P** layer were determined to be 62 ± 1 and 20 ± 1 Å, respectively; therefore, the concentration of $W_{10}O_{32}^{4-}$ in the S-(**P**/**W**)$_n$ films was calculated to be 1.0×10^{-3} M. Similarly, the thickness of a S-(**P**/**W**)$_{11}$/**P** film, self-assembled onto an ITO-coated glass substrate, was evaluated to be 240 Å. The thickness of a **P**/**W** unit and the concentration of $W_{10}O_{32}^{4-}$ in the S-(**P**/**W**)$_n$ films on the ITO surface were calculated to be 23 Å and ca. 0.9×10^{-3} M, respectively. It is suggested that the concentration of $W_{10}O_{32}^{4-}$ in the

(42) Fuchs, V. J.; Hartl, H.; Schiller, W.; Gerlach, U. *Acta Cryst.* **1976**, *B32*, 740.

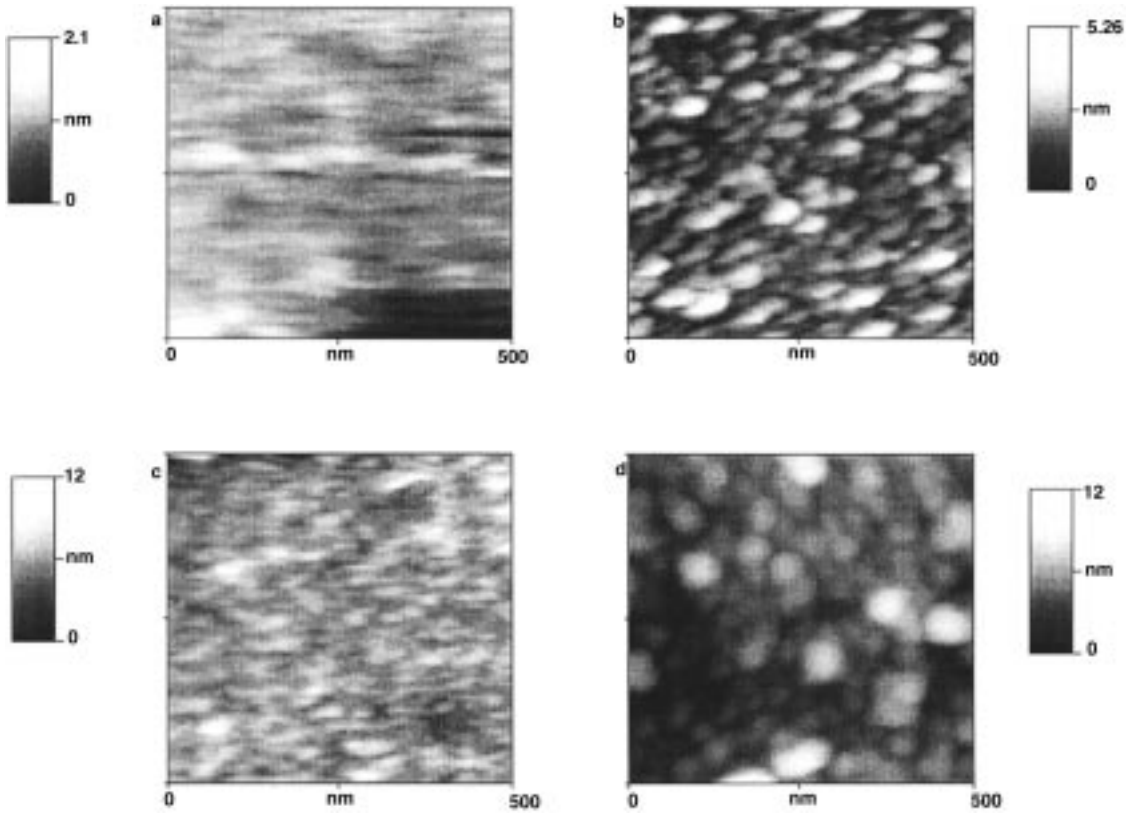

Figure 5. AFM images of one layer of **P** (a) and of self-assembled S-(**P**/**W**)$_n$ films with $n = 1$ (b) and $n = 2$ (d) and of a self-assembled S-(**P**/**W**)$_1$/**P** film (c) on mica substrates.

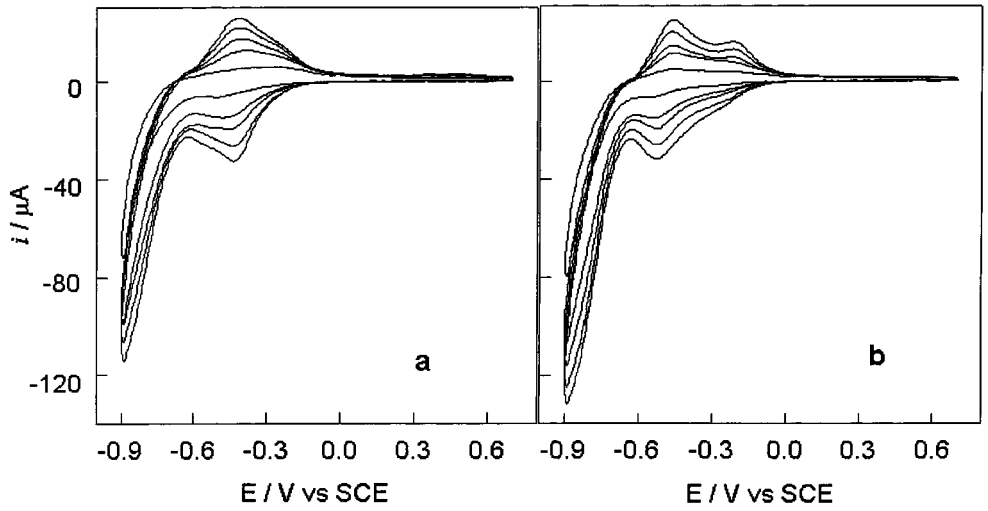

Figure 6. Cyclic voltammograms self-assembled S-(**P**/**W**)$_n$ (a) and self-assembled S-(**P**/**W**)$_n$/**P** films (b) with increasing number of *n*'s (paralelling the increase of current values) in aqueous 0.10 M NaCl at pH = 2.5.

S-(**P**/**W**)$_n$ films is almost constant irrespective of the kind of substrates used; thus the difference in absorbance of the S-(**P**/**W**)$_n$ films is due to film thickness. The difference of film thickness can be ascribed to the adsorption of the first **P** layer on the substrate at pH = 2.5, the amount of which depends on charge density, isoelectric point, and surface roughness.

The topography of mica-supported S-(**P**/**W**)$_n$ films was investigated by AFM. The first layer of **P** (S-**P**) showed a featureless AFM image with a height variation of about 2 nm (Figure 5a), consistent with films that have been reported previously.[24] Adsorption of **W** onto the (S-**P**) film manifested itself in the formation of numerous domains with a height variation of around 4 nm (Figure 5b). Self-assembly of the second layer of **P** to form the S-(**P**/**W**)/**P** film decreased the height variation to below 3 nm (Figure 5c), and adsorption of a layer of **W** to produce S-(**P**/**W**)$_2$ resulted in the same type of domains (Figure 5d) as was imaged in Figure 5b. Adsorption of **W** is seen to transform the relatively smooth surface of the **P** layer to a loopy brush-like structure in which the high ionic strength ($I > 0.2$) **W** associate **P** ($I \approx 0.02$) to a complex ion pair with a relatively rough surface. These observations support the schematics drawn for the self-assembly of a S-(**P**/**W**)$_n$ film (Figure 1).

Cyclic Voltammetry. Cyclic voltammograms of an aqueous 10 mM **W** solution (at pH = 2.5, using a bare

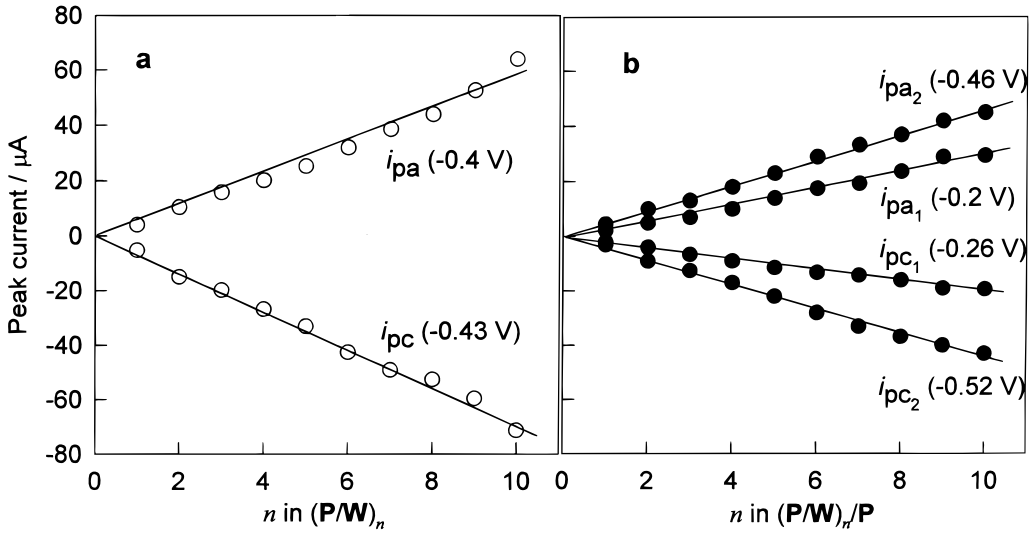

Figure 7. Dependence of peak current on n in self-assembled S-(**P**/**W**)$_n$ (a) and self-assembled S-(**P**/**W**)$_n$/**P** films (b).

Pt) showed two redox waves at $E_1^{o\prime} = -0.16$ V ($E_{pc1} = -0.19$ V, $E_{pa1} = -0.13$ V) and $E_2^{o\prime} = -0.4$ V ($E_{pc2} = -0.48$ V, $E_{pa2} = -0.32$ V). The potential of the first cathodic peak (E_{pc1}) was consistent with the reported value for **W** ($E_{pc1} = -0.19$ V),[40] and its peak current was proportional to the square root of the sweep rate (v) in the range of 5−200 mV s^{-1} as expected for a diffusion-limited process. The second redox wave with $E_2^{o\prime} = -0.4$ V, associated with H_2 evolution, had a large current and shifted from that reported for **W** ($E_{pc2} = -0.34$ V). When a bare ITO electrode was used as a working electrode, the CV measurements of an aqueous 10 mM **W** solution (at pH = 2.5) showed two 1e redox waves at $E_1^{o\prime} = -0.18$ V ($E_{pc1} = -0.28$ V, $E_{pa1} = -0.08$ V) and $E_2^{o\prime} = -0.4$ V ($E_{pc2} = -0.52$ V, $E_{pa2} = -0.28$ V) at v of 50 mV s^{-1}. The two anodic peaks changed into one broad peak which shifted positively from the reported value[40] with a multiple scan and/or an increase in v. The irreversible behavior was due to the strong adsorption of 2e-reduced species of **W** ($W_{10}O_{32}^{6-}$ or $H_2W_{10}O_{32}^{4-}$) on the electrode surface. The slow disappearance of the blue color, due to the reduced species of **W**, during the potential sweep toward positive is in accord with this postulate.

Cyclic voltammograms (in 0.1 M aqueous NaCl at pH = 2.5) of the S-(**P**/**W**)$_n$ and S-(**P**/**W**)$_n$/**P**, self-assembled onto ITO-coated glass working electrodes, showed peak currents which were proportional to v in the range of 5−200 mV s^{-1}. The number and potential of the redox waves depended, however, on the chemical composition of the last (the outermost) layer of the self-assembled film (i.e., whether it was **W** or **P**) as shown in Figure 6. The S-(**P**/**W**)$_n$-modified electrode (i.e., **W** is the outermost layer) showed a redox wave at $E^{o\prime} = -0.415$ V ($E_{pc1} = -0.43$ V, $E_{pa1} = -0.4$ V). Conversely, the S-(**P**/**W**)$_n$/**P** modified electrode (i.e., **P** is the outermost layer) underwent two 1e redox waves at $E_1^{o\prime} = -0.23$ V ($E_{pc1} = -0.26$ V, $E_{pa1} = -0.2$ V) and $E_2^{o\prime} = -0.49$ V ($E_{pc1} = -0.52$ V, $E_{pa1} = -0.46$ V).

The difference of redox potentials from that reported for **W** ($E_{pc1} = -0.19$ V, $E_{pa1} = -0.34$ V)[40] is likely to be due to the strong interaction between the$W_{10}O_{32}^{4-}$ (oxidized species) and the cationic **P** molecules. The

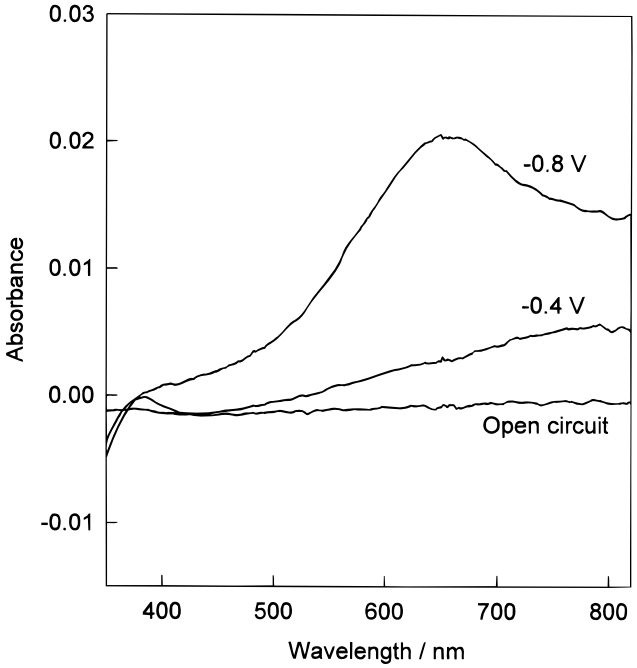

Figure 8. Absorption spectra of a self-assembled S-(**P**/**W**)$_6$/**P** film at 0, −0.4, and −0.8 V applied potentials.

peak area of the redox wave due to S-(**P**/**W**)$_n$ was consistent with the sum area of the two redox waves of S-(**P**/**W**)$_n$/**P**, indicating that a direct 2e$^-$ redox occurred in the S-(**P**/**W**)$_n$ film. This was also confirmed by absorption spectrophotometry. Observations of a single 2e$^-$ redox wave for the $HN(Bu)_3^+$ salt of $W_{10}O_{32}^{4-}$ and for $SiW_{12}O_{40}^{4-}$ at low pH were rationalized in terms of formation of a protonated species, $HW_{10}O_{32}^{4-}$.[41,43] We consider that protons play an important part in the charge compensation during cyclic votammetry of the self-assembly films; for example, protons are easily incorporated at the reduction process. However, the incorporation of protons in an S-(**P**/**W**)$_n$/**P** film is suppressed. In both the S-(**P**/**W**)$_n$ and S-(**P**/**W**)$_n$/**P** films, peak currents increased linearly with the increase in n

(43) Keita, B.; Nadjo, L. *J. Electroanal. Chem.* **1987**, *217*, 287.

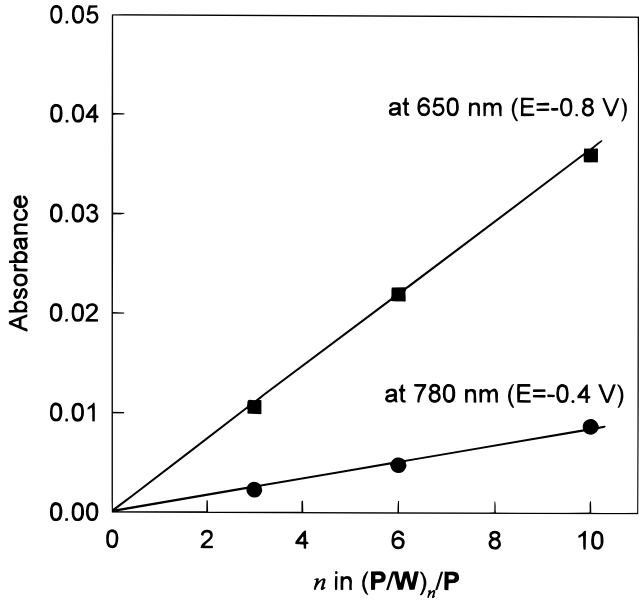

Figure 9. Dependence of the absorbances at 650 and 780 nm on n in self-assembled S-(**P**/**W**)$_n$/**P** films during coloration.

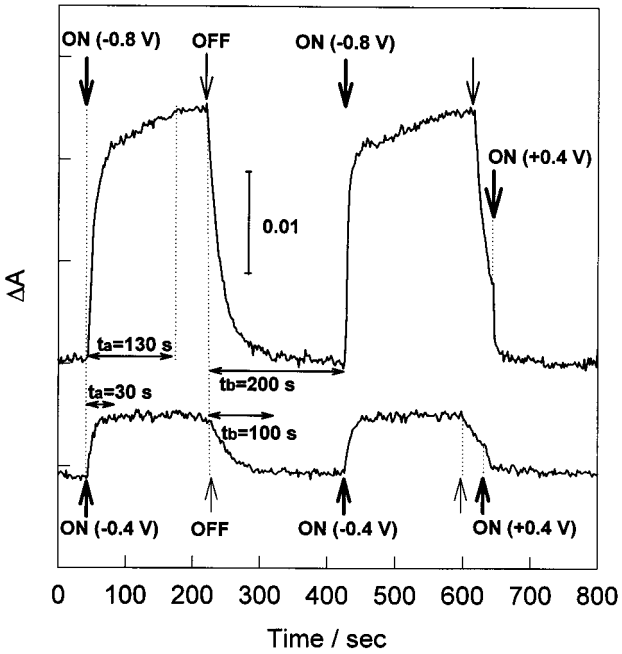

Figure 10. Absorbance changes at 650 nm (−0.8 V) and 780 nm (−0.4 V) in a self-assembled S-(**P**/**W**)$_6$/**P** film accompanying the potential steps of 0 → −0.4 V; 0 → −0.8 V; 0 → +0.4 V; and 0.8 → +0.4 V. t_a and t_b are response times for coloration and bleaching, respectively.

(see Figure 7). On the basis of the geometric area of the ITO electrode and integrating the area under the $i-E$ curves, the amount of **W** per one adsorption process was determined to be ca. 2×10^{-10} mol cm^{-2} and indicates that all of $\mathbf{W}_2$ incorporated into the self-assembly films is electrochemically active.

Electrochromic Behavior. The observed color change during the cyclic voltammetry of **W** in an aqueous acidic solution originates in the presence of an intervalence charge-transfer band ($W^V-O-W^{VI} \leftrightarrow W^{VI}-O-W^V$) which is readily influenced by an applied potential and/or light and hence it manifests itself in electrochromism and/or photochromism:[35,38]

Table 1. Response Times of Coloration (t_c) and Bleaching (t_b) for S-(P/W)$_n$/P Films

		n		
	potential step	3	6	10
t_c/s	0 → −0.4 V	20 (3)[a]	45 (10)	50 (15)
	0 → −0.8 V	100 (5)	130 (15)	180 (20)
t_b/s	0 → −0.4 V	80 (35)	100 (50)	180 (60)
	0 → −0.8 V	160 (65)	200 (70)	300 (80)

[a] Values in parentheses are mean response times, obtained from 80% absorbance changes.

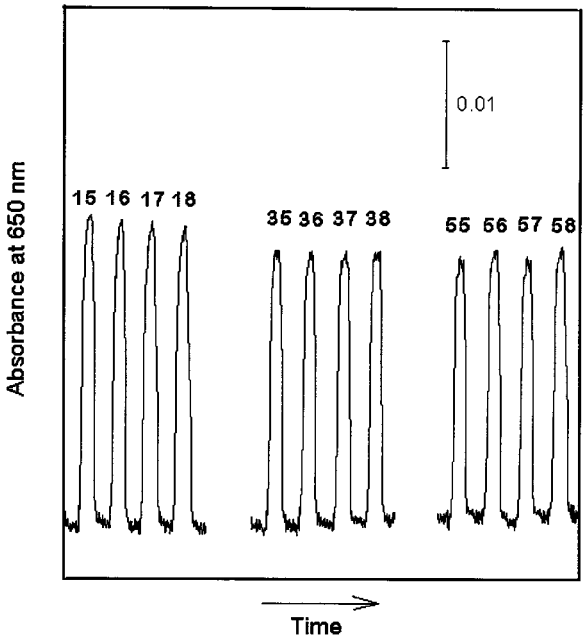

Figure 11. Absorbance changes at 650 nm in a self-assembled S-(**P**/**W**)$_6$/**P** film during repeated potential steps (the numbers indicate the number of steps after which the spectra were taken).

$$\underset{\text{(colorless or pale yellow)}}{W_{10}O_{32}^{4-}} + e^- + H^+ \leftrightarrow \underset{\text{(pale blue)}}{HW_{10}O_{32}^{4-}} \quad (1)$$

$$\underset{\text{(pale blue)}}{HW_{10}O_{32}^{4-}} + e^- + H^+ \leftrightarrow \underset{\text{(dark blue)}}{H_2W_{10}O_{32}^{4-}} \quad (2)$$

Electrochromism was investigated for the S-(**P**/**W**)$_n$/**P** (n = 3, 6, 10) films by absorption spectrophotometric measurements during application of different potentials by chronoamperometry. Absorption spectra of a S-(**P**/**W**)$_6$/**P** film self-assembled onto an ITO-coated glass electrode at applied potentials of 0 V (open circuit), −0.4 V, and −0.8V are illustrated in Figure 8. The absorption peaks around 780 and 650 nm, corresponding to the 1e$^-$ reduced ($HW_{10}O_{32}^{4-}$) and 2e$^-$ reduced ($H_2W_{10}O_{32}^{4-}$) species, were observed at −0.4 and −0.8 V, respectively. Films S-(**P**/**W**)$_3$/**P** and S-(**P**/**W**)$_{10}$/**P** behaved analogously. Absorbances at 780 and 650 nm increased with the increase of n in S-(**P**/**W**)$_n$/**P** (Figure 9). The amount of 2e$^-$ reduced species ($H_2W_{10}O_{32}^{4-}$) per one **W**-layer were calculated to be 1.8×10^{-10} mol cm^{-2} by using the molar absorbance (ϵ = 18 000).[35] This value is in good agreement with those assessed from the absorption spectra at 324 nm (2.1×10^{-10} mol cm^{-2}) and from the areas in the cyclic voltammetry (2.0×10^{-10} molcm^{-2}), indicating that almost all of **W** self-assembled in the ultrathin films contributed to the electrochromism. On the other hand,

S-(**P**/**W**)$_n$ films showed the adsorption of $2e^-$ reduced species without that of $1e^-$ reduced species during the reduction.

Typical time courses of absorbances of the S-(**P**/**W**)$_6$/**P** film, at 780 and 650 nm, during potential-step chronoamperometry (0 V → −0.4 V, 0 V → −0.8 V) are illustrated in Figure 10. The response times for the coloration processes by applying −0.4 and −0.8 V were shorter than those for the bleaching by turning off the voltage (open circuit). The response times of coloration (t_c) and bleaching (t_b) for S-(**P**/**W**)$_n$/**P** films increased with an increase of n (see Table 1). The t_b for all samples could be changed to be fairly shorter by applying the voltage of +0.4 V after potential steps of 0 V → −0.4 and 0 V → −0.8 V as shown in Figure 10.

Recycling the potential-dependent color changes was investigated on the S-(**P**/**W**)$_6$/**P** film by recording the absorbance at 650 nm during repeating the potential-step cycle of +0.4 V ↔ −0.8 V 60 times (Figure 11). The reproducibility of the optical responses (within a ±5% error throughout multiple cycling of the potential steps) demonstrates a stable electrochromic property of the self-assembled S-(**P**/**W**)$_n$/**P** films.

Conclusion

Construction of ultrathin electrochromic S-(**P**/**W**)$_n$/**P** films by the layer-by-layer self-assembly of poly(diallyldimethylammonium) chloride and sodium decatungstantate is the most significant accomplishment of the present work. The relative ease and versatility of the self-assembly opens the door to the fabrication of related devices with nanolevel control.

Acknowledgment. This study was supported by The Foundation of Kyushu Industrial Technology Center in Japan.

CM980127B